arXiv:cond-mat/0202347v1 [cond-mat.str-el] 20 Feb 2002

Giant infrared intensity of the Peierls mode at the neutral-ionic phase transition

Luca Del Freo and Anna Painelli*
Dip. di Chimica GIAF Università di Parma, I–43100 Parma, Italy; INSTM UdR Parma

Z.G.Soos
Dept. of Chemistry, Princeton University, Princeton, New Jersey 08544
(Dated: November 10, 2021)

We present exact diagonalization results on a modified Peierls-Hubbard model for the neutral-ionic phase transition. The ground state potential energy surface and the infrared intensity of the Peierls mode point to a strong, non-linear electron-phonon coupling, with effects that are dominated by the proximity to the electronic instability rather than by electronic correlations. The huge infrared intensity of the Peierls mode at the ferroelectric transition is related to the temperature dependence of the dielectric constant of mixed-stack organic crystals.

PACS numbers: 78.30.Jw, 63.20.Kr, 74.25.Kc

The nature of electron-phonon (e-ph) coupling in correlated electron systems is an enduring topic in condensed matter research, currently as experimental indications of strong, anharmonic e-ph coupling have been recognized in high-T_c superconductors based on CuO [1] or the novel MgB_2 [2]. The topic itself is old and deeply rooted in the problem of structural deformation in systems close to electronic instabilities, where particularly high sensitivity to e-ph coupling is expected. Low-dimensional systems have a host of electronic instabilities such as Mott, Peierls, and spin-Peierls transitions [3] with characteristic vibrational signatures [4]. All these instabilities are accompanied by lattice relaxation representing the extreme consequence of the non-linearity of electronic responses to perturbation by phonons.

The neutral-ionic transition (NIT) in a rigid donor-acceptor (DA) chain is the boundary between a paramagnet and a diamagnet [5], analogous to a Mott metal-insulator transition. Such electronic instability is again accompanied by structural relaxation. NITs were observed in organic charge-transfer (CT) crystals with mixed DA stacks [6], and, as recognized from the outset [7], dimerization accompanies the transition, leading to ferroelectric (FE) behavior [8] for proper interstack arrangement. Recently NIT models were proposed for FE oxides [9]. In this context the anomalous role of dimerization in displacing electronic charge has been underlined, to suggest enhanced e-ph coupling near the NIT. This was confirmed by subsequent calculations [10] without, however, pursuing experimental implications.

In this Letter, we exploit the recent definition [10, 11] of polarization, P, in insulators with periodic boundary conditions (PBC) to obtain the infrared (IR) intensity of the dimerization mode. The IR intensity depends sensitively on structure, which we relax fully, and peaks at the FE transition of either correlated or uncorrelated models, clearly implicating the structural instability rather than correlations for the huge intensity. Working with a *linear* and *harmonic* model for e-ph coupling, we recognize large non-linearity in the anharmonicity of the ground state (GS) potential energy surface (PES), and within the *adiabatic* approximation we demonstrate an intimate entanglement of electrons and phonons. Sizeable non-adiabatic effects are expected near the NIT [12], but the subtle interplay between electrons and phonons we discuss here sets the baseline for identifying non-adiabatic effects.

We describe NIT in terms of a Peierls-Hubbard model with alternating on-site energies (Δ) and one electron per site. As in the Su-Schrieffer-Heeger (SSH) model [13], linear Peierls coupling to a $k = 0$ phonon that modulates the transfer integrals is introduced in the following adiabatic Hamiltonian:

$$\mathcal{H} = -\sum_{i,\sigma}\left(1+(-1)^i\delta\right)\left(c^\dagger_{i,\sigma}c_{i+1,\sigma}+h.c.\right) + U\sum_i n^\dagger_{i,\sigma}n_{i,\sigma'} + \Delta\sum_{i,\sigma}(-1)^i c^\dagger_{i,\sigma}c_{i,\sigma} + \frac{N}{2\epsilon_d}\delta^2 \quad (1)$$

where N is the number of sites, $c^\dagger_{i,\sigma}$ creates an electron with spin σ on site i, and the last term accounts for the elastic energy. Accounting for alternating charges on molecular cores, q_j=2, 0 on D, A sites, respectively, we define the ionicity operator as $\hat{\rho} = \sum_j (q_j - \hat{n}_j)/N$.

For $\Delta = 0$ Eq. (1) reduces to the SSH model [13] in the $U = 0$ limit, or to a spin-Peierls model in the $U >> 1$ limit, and the Peierls instability leads to finite dimerization amplitude, δ, in either case. The I phase with one electron per site ($\rho \sim 1$) is always dimerized [14, 15]. With increasing Δ, electrons are paired on $-\Delta$ sites in the N phase and the GS is a regular chain ($\delta = 0$). The equilibrium δ decreases with Δ and vanishes for Δ larger than a critical value that depends on the lattice stiffness, as shown by Rice and Mele for $U = 0$ [16]. The correlated case is a Mott insulator on the I side [17], with an NIT to a band insulator around $\Delta \sim U/2$ in the regular chain. Accordingly, we vary $\Gamma = \Delta - U/2$ in the vicinity of the

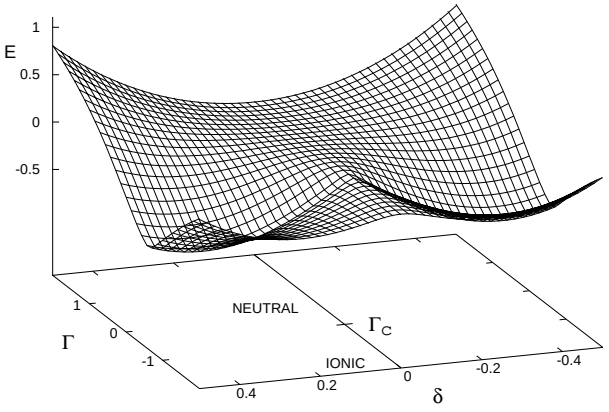


FIG. 1: The GS energy of a 12 site ring with $\epsilon_d = 0.64$.

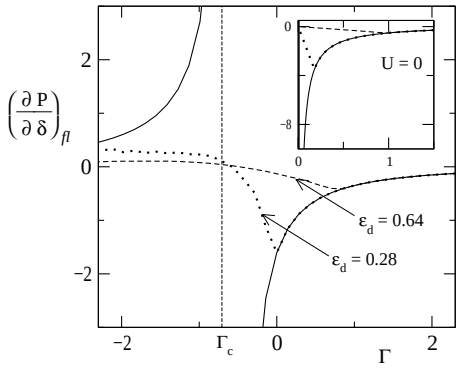


FIG. 2: The fluctuating charge contribution to $\partial P/\partial\delta$, calculated for $N = 12$ and $U = \infty$. Continuous line refers to the regular chain. Dotted and dashed lines refer to the equilibrium dimerization starting at the intersection with the continuous line. The inset shows results for $U = 0$ and $N = \infty$.

NIT and solve $\mathcal{H}(\Gamma, \epsilon_d)$ exactly in the limit $\Delta, U \to \infty$ for finite chains with up to 12 sites and PBC, as required for the P operator [11], using the diagrammatic valence bond (VB) technique [18]. The lengthy geometry optimization limits N, but is compensated by the rapid convergence of GS properties compared to excitation energies [17].

In the rigid lattice ($\epsilon_d = 0$) ρ varies smoothly and the N-I crossover, at $\Gamma_c = -0.668$ and $\rho \sim 0.63$, is signaled by the unconditional dimerization instability of the I phase [17]. A deformable lattice (finite ϵ_d) dimerizes on the N side [15]. Fig. 1 depicts the evolution with Γ of the GS PES of a 12-site ring with $\epsilon_d = 0.64$. To focus attention on dimerization, the GS energy for the regular chain is set to zero at each Γ. Far in the N phase (large positive Γ) the regular stack is stable, but with decreasing Γ, dimerization sets in well before Γ_c, at $\rho \sim 0.25$. In the pre-transitional regime the GS PES is clearly anharmonic. The two minima in the I regime correspond to ferroelectrics with opposite polarization.

To calculate the IR intensity of the Peierls mode, proportional to $(\partial P/\partial\delta)^2$, we slightly modify the Resta's twist operator [11], to account for alternating charges on molecular cores, as follows:

$$P = \frac{1}{2\pi} Im(ln\langle\Psi|e^{i\frac{2\pi}{N}\hat{M}}|\Psi\rangle) = \frac{1}{2\pi} Im(ln(Z)) \quad (2)$$

where Ψ is the GS wavefunction, and $\hat{M} = \sum_j r_j(q_j - \hat{n}_j)$, with r_j locating the j site. The $\hat{M}$-operator is diagonal in the VB basis and the calculation of P is easily implemented. $\hat{M}$ accounts for the actual geometry of the stack and depends on δ according to:

$$\hat{M} = \frac{N^2}{2} - \sum_j j\hat{n}_j + \frac{N\delta}{2\alpha}\hat{\rho} \quad (3)$$

where the mean intersite distance and the electronic charge are set to 1. The dimensionless e-ph coupling constant, $\alpha = \sqrt{K\epsilon_d}$, is estimated $\sim$ 5-10, for typical values of the elastic constant, K. $\partial P/\partial\delta$ can be rigorously decomposed into two contributions, one obtained by allowing M to vary with δ, at fixed Ψ, the other one by varying Ψ at fixed M. The first contribution describes the IR intensity originating from the displacement of sites carrying a fixed charge, ρ. Frozen charges account for IR intensity of optical modes in ionic lattices. The second, electronic contribution instead accounts for the charge flux driven by δ. It only appears in systems with mobile or delocalized electrons.

For a regular chain, $\delta = 0$, the reflection mirror residing on each site ensures real Z values [11]. Z is positive in the N regime, negative in the I regime, and $Z = 0$ locates the NIT of a $\delta = 0$ ring of any size with PBC [10]. The δ derivative of P in Eq. (2) then diverges at the NIT, where the GS is metallic [17]. In dimerized chains Z is complex and the divergence of $\partial P/\partial\delta$ is suppressed. Since the GS of Eq. (1) always dimerizes on the N side of the NIT, the IR intensity remains finite for the equilibrium structure. The IR intensity of the regular chain is then an upper bound for the relaxed structure that, depending on ϵ_d, holds on the N side of the FE transition.

We numerically evaluate $\partial P/\partial\delta$ at the equilibrium δ and distinguish between contributions due to fluctuating and frozen charges. The latter is small in the entire range of Γ. Large IR intensity is associated with fluctuating charges. Fig. 2 shows $(\partial P/\partial\delta)_{fl}$ for 12-site chains. The $\delta = 0$ curve diverges at Γ_c on both the N and I side. Giant IR intensity at the NIT is due to finite electronic fluxes generated by infinitesimal lattice distortions. Resta and Sorella reported similar results by finding the total average charge for fixed dimerization [10]; for small δ, their quasi-divergent curves are finite-difference approximations to our δ-derivatives. We see in Fig. 2 that $(\partial P/\partial\delta)_{fl} = 0$ near Γ_c for both values of ϵ_d. Dimerization increases the transfer integral $(1 + \delta)$

and tends to equalize charges on D and A sites then producing charge fluxes of opposite direction on the N and I side. $(\partial P/\partial\delta)_{fl} = 0$ marks the point where charges are maximally delocalized and locates the N-I crossover in dimerized chains.

Since Mott insulators on the I side are inherently correlated, all NIT features have been viewed in terms of correlations, including the divergence of dynamical charges at the NIT of the regular chain [10]. To address this point we investigated the non-interacting case, and found $P(\Delta, \delta, U = 0)$ analytically for the infinite chain:

$$P(\Delta, \delta, U = 0) = \frac{\delta\rho}{2\alpha} - \frac{4\delta}{\pi\Delta\sqrt{\Delta^2+4}} cel(q_c, p, a, b) \quad (4)$$

where $cel(q_c, p, a, b)$ is the complete elliptic integral of the third kind [19], calculated for $q_c^2 = (\Delta^2 + 4\delta^2)/(\Delta^2 + 4)$, $p = (\Delta^2 + 4\delta^2)/(\Delta^2)$, $a = 1$, and $b = 0$. For the regular chain the δ-derivative of ρ and of the elliptic integral above both vanish so that the frozen and the fluctuating charge contributions to $\partial P/\partial\delta$ are the coefficients of δ in the first and second term of Eq. (4), respectively. For typical α values the frozen charge contribution smoothly increases from 0 to ~ 0.05 as ρ increases from 0 to 1. The fluctuating charge contribution is more interesting and is shown in the inset of Fig. 2 for positive Δ ($\Delta < 0$ simply reverses the role of D and A). $(\partial P/\partial\delta)_{fl}$ diverges as $\Delta \to 0$, much as it does for $U = \infty$ at NIT. Indeed, Eq. (1) at $U = \Delta = 0$ describes the half-filled band whose instability Peierls pointed out, and $\Delta = 0$ is the NIT for free electrons. We conclude that divergent IR intensity at the FE transition is not due to electronic correlations, but rather indicates a structural instability that displaces electronic charges. The behavior of chains with finite ϵ_d at the equilibrium dimerization (dashed and dotted lines in the inset) in the N phase is similar to the $U = \infty$ case, with $(\partial P/\partial\delta)_{fl}$ vanishing at $\Delta = 0$ and at Γ_c, respectively.

Fig. 3 shows results for Peierls coupling $\epsilon_d = 0.28$ and 0.64 in Eq. (1) with $U = \infty$. The larger dimerization for $\epsilon_d = 0.64$ strongly localizes electrons and reduces finite-size effects: rings of 10 and 12 sites appear superimposed, while they show small differences for ϵ_d =0.28. The IR intensity is dominated by fluctuating charges; it is small far in the N regime, peaks sharply at the FE transition, and decreases rapidly to vanish at the N-I crossover. In fact, since the frozen charge contribution is small, vanishing IR intensity can be taken as an operational definition of the charge crossover. The IR intensity smoothly increases again on the I side due to the increasing frozen charges and reaches typical values for ionic crystals as $\rho \to 1$. The peak in the IR intensity at the FE transition is larger the nearer the transition is to the NIT of the regular chain, where electronic charges are most responsive. IR intensity does not measure the strength of e-ph coupling, nor the dimerization amplitude, rather it

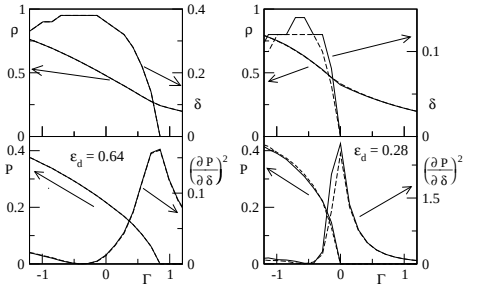


FIG. 3: GS equilibrium ionicity, dimerization amplitude, polarization and IR intensity for $U = \infty$ and two different ϵ_d. Note the scale change for both δ and $(\partial P/\partial\delta)^2$. Continuous and dashed lines refer to N=12 and 10, respectively (the two curves coincide in the left panels).

is governed by the response of the electronic system and reflects its non-linearity.

The Peierls-Hubbard model in Eq. (1) contains neither intersite electron-electron interactions nor coupling to molecular (Holstein) modes. Consequently it cannot describe materials such as TTF-CA [7] with a discontinuous NIT. But Eq. (1) provides a useful starting point for systems with a continuous NIT, or, more precisely, a dimerization transition near a continuous NIT. Several CT salts dimerize in the N regime [20, 21, 22] with decreasing temperature or increasing pressure; this modulates Γ through the crystal's Madelung energy. Far IR data on these systems are however scanty, the only available results having recently been published on TTF-$QBrCl_3$ [22]. This compound has $\rho \sim 0.3$ at ambient conditions and dimerizes at T$\sim$ 68 K. Concomitantly, its ionicity increases from ~ 0.35 to 0.5 to reach ~ 0.6 at T $\sim$ 10K. Reflectivity measured at the lowest frequency (25 cm^{-1}) increases up to 90% at the FE transition, suggesting the proximity to a metallic state there. After dimerization, the reflectivity decreases again. Approaching the FE transition, a progressive displacement of the IR intensity towards lower frequencies can be inferred from data in Ref. [22], and the published IR intensity vs. T closely resembles the $\epsilon_d = 0.28$ peak in Fig. 3. Therefore we assign the amplified far IR intensity observed near the FE transition to the soft dimerization mode, and explain its abrupt drop after the transition as due to the vanishing of the fluctuating contribution to the IR intensity at the N-I crossover. This interpretation differs from the one proposed in Ref. [22], where the far-IR absorption is assigned to the dynamics of neutral-ionic domain-walls. Additional experimental and theoretical work is needed to clarify this point.

There are more data on static dielectric constants, ε [21, 22]. Systems undergoing dimerization near a continuous NIT show a large peak in ε just where long-range dimerization sets in. The similarity between the ε peak (see e.g. Fig. 1 in ref. [22]) at the FE transition and the IR intensity of the Peierls mode in Fig. 3 is sugges-

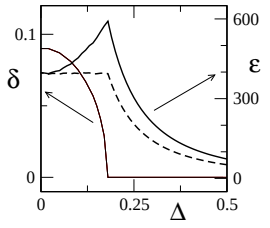


FIG. 4: The equilibrium dimerization and dielectric constant for $U = 0$ and $\epsilon_d = 0.28$. Dashed and continuous line refer to the purely electronic and to the total ε, respectively.

tive. E-ph coupling shifts oscillator strength from electronic states to lattice vibrations, and this displacement to lower energy amplifies the system's response to a static field.

To the first order in ϵ_d, the static response can be estimated as the sum of an electronic plus a vibrational contribution: $\varepsilon = 1 + (\chi_{el} + \chi_{vib})/\varepsilon_0$, with $\chi_{vib} = 2\mu_{IR}^2/\omega \propto \epsilon_d(\partial P/\partial\delta)^2$, defined in terms of the vibrational transition dipole moment and frequency [23]. Analytical expressions of χ_{el} are available for $U = 0$ [24], and Fig. 4 compares the total (electronic+vibrational) ε with the purely electronic term. The lattice parameters, required to fix the absolute value of ε, are set to representative values for mixed stack crystals from Ref. [25]. Whereas the magnitude of the two terms is comparable, the sharp peak at the FE transition is due e-ph coupling. Again our interpretation differs from that in Ref. [22], where the amplification of the dielectric constant at the FE transition was related to the frequency of the far IR mode, via the Lyddane-Sachs-Teller relation. We instead underline the role of the dimerization mode in displacing electronic charges. Consistent with available data [21, 22], we predict large ε peaks at FE transitions occurring at intermediate ρ, i.e. for systems that, due to either small Peierls coupling or to disorder, undergo dimerization very close to the electronic (NIT) instability. Preliminary ε calculations on $U = \infty$ open chains yield similar results, suggesting once more that the physics of FE transitions has more to do with phonons than with electronic correlations.

Experimental evidence is accumulating for strong e-ph coupling in high-T_c superconductors [1, 2]. The proximity to an electronic instability is a unifying features of exotic superconductivity in cuprates, organics, or MgB_2, as well as IR intensity or dielectric responses of CT salts. Using an *adiabatic* model for an extended electronic system with an electronic instability, we demonstrate here that, quite irrespective of electronic correlations, *linear* e-ph coupling, *harmonic* phonons and delocalized electrons produce large and non-linear effects originating from a complex interplay of electronic and nuclear degrees of freedom.

We thank Italian MIUR and CNR for supporting work in Parma; partial support from NSF through MRSEC program is acknowledged for work in Princeton.

* Electronic address: anna.painelli@unipr.it

[1] A.Lanzara *et al.*, Nature, **412**, 510 (2001); R. J. McQueeney, *et al.*, Phys. Rev. Lett. **87**, 77001 (2001).
[2] T. Yildirim, *et al*, Phys. Rev. Lett. **87**, 37001 (2001); K.-P.Bohnen, *et al*, Phys. Rev. Lett. **86**, 5771 (2001); A.Y.Liu, *et al*, Phys. Rev. Lett. **87**, 87005 (2001)
[3] D.Baeriswyl, *et al*, in *Conducting Polymers*, edited by H.Kiess (Springer-Verlag, Heidelberg, 1992), p. 7
[4] R.Bozio and C.Pecile, in *Advances in Spectroscopy*, vol. 19 (wiley, New York, 1991) p.1, and references therein.
[5] Z.G.Soos, *et al*, Chem. Phys. Lett., **65**, 331 (1979).
[6] J.B. Torrance, *et al*, Phys. Rev. Lett., **46**, 253 (1981); **47**, 1747 (1981).
[7] A.Girlando, *et al*, J. Chem. Phys., **79**, 1075 (1983).
[8] S. Horiuchi, *et al*, J. Am. Chem. Soc., **120**, 7379 (1998).
[9] T. Egami, *et al*, Science, **261**, 1307 (1993).
[10] R.Resta and S.Sorella, Phys. Rev. Lett., **74**, 4738 (1995).
[11] R.Resta, Rev. Mod. Phys. **66**, 899 (1994).
[12] G.P.Borghi, *et al*, Europhys. Lett., **34**, 127 (1996);
[13] A.J.Heeger, *et al*, Rev. Mod. Phys. **60**, 781 (1988).
[14] N.Nagaosa, J.Phys.Soc.Jpn, **55**, 2754 (1986); **55** 3488 (1986).
[15] A.Painelli, and A.Girlando, Phys. Rev. B, **37**, 5748 (1988).
[16] M.J.Rice, and E.J.Mele, Phys. Rev. Lett., **49**, 1455 (1982).
[17] Y.Anusooya-Pati, *et al*, Phys. Rev. B, **63**, 205118 (2001); and references therein.
[18] Z.G.Soos and S.Ramasesha, in *Valence Bond Theory and Chemical Structure*, edited by D.J.Klein and N.Trinajstic (Elsevier, New York, 1990), p. 81.
[19] W.H.Press, *et al.*, *Numerical Recipes*, Cambridge University Press, Cambridge (1986).
[20] A.Girlando, *et al.*, J.Chem.Phys. **98**, 7692 (1993); M.Masino *et al.*, Phys.Chem.Chem.Phys. **3**, 1904 (2001); L.Farina, *et al.*, Phys. Rev. B **64**, 144102 (2001).
[21] S. Horiuchi, *et al.*, J.Am.Chem.Soc. **123**, 665 (2001).
[22] Y.Okimoto, *et al*, Phys. Rev. Lett., **87**, 187401 (2001).
[23] A.Painelli, Chem.Phys.Lett., **285**, 352 (1998)
[24] C.Cojan, *et al.*, Phys.Rev.B **15**, 909 (1977).
[25] M. Le Cointe, *et al.*, Phys. Rev. B **51**, 3374 (1995).